Caveolin Moves from Caveolae to the Golgi Apparatus in Response to Cholesterol Oxidation

Eric J. Smart, Yun-Shu Ying, Patricia A. Conrad, and Richard G. W. Anderson

Department of Cell Biology and Neuroscience, University of Texas Southwestern Medical Center, Dallas, Texas 75235

Abstract. Caveolae are a membrane specialization used to internalize molecules by potocytosis. Caveolin, an integral membrane protein, is associated with the striated coat present on the cytoplasmic surface of the caveolae membrane. We now report that oxidation of caveolar cholesterol with cholesterol oxidase rapidly displaces the caveolin from the plasma membrane to intracellular vesicles that colocalize with Golgi apparatus markers. After the enzyme is removed from the medium, caveolin returns to caveolae. When untreated cells are gently homogenized, caveolin on the plasma membrane is accessible to both anti-caveolin IgG and trypsin. After cholesterol oxidase treatment, however, Golgi-associated caveolin is inaccessible to both of these molecules. Brefeldin A, which inhibits ER to Golgi trafficking, blocks the appearance of caveolin in the Golgi apparatus but does not prevent caveolin from leaving the plasma membrane. Indirect immunogold localization experiments show that in the presence of cholesterol oxidase caveolin leaves the plasma membrane and becomes associated with endoplasmic reticulum and Golgi compartments. Surprisingly, the loss of caveolin from the plasma membrane does not affect the number or morphology of the caveolae.

CAVEOLAE are a membrane specialization found on the surface of many different cells (23, 36). There is considerable evidence that they are an endocytic organelle that internalizes substances by forming plasmalemmal vesicles (24). In some cases these vesicles transport molecules across the cell (32) while at other times they deliver low molecular weight molecules and ions to the cytoplasm by a process called potocytosis (1). The cytoplasmic surface of each caveola is decorated with a characteristic coat material that appears to be composed of integral membrane components (28). One of the proteins associated with this coat is caveolin (28). The caveolae coat may play a role in controlling membrane invagination.

Potocytosis was discovered by studying receptor-coupled transport of folate in MA104 cells (15). At physiological concentrations of 5-methyltetrahydrofolate, the efficient delivery of the vitamin to the cytoplasm of cells is dependent on a high affinity receptor that is anchored to the membrane by glycosylphosphatidylinositol (GPI)[1]. The GPI-anchor causes the receptor to cluster in caveolae (30) where it becomes sequestered from the extracellular space each time a caveolae closes. Sequestered folate rapidly dissociates from the receptor and crosses the membrane by an anion carrier (16). Caveolae then open and another round of potocytosis begins. Recently we showed (34) that activators of protein kinase C (PKC) inhibit potocytosis by preventing the invagination of caveolae.

Caveolin was originally identified as a 22-kD tyrosine phosphoprotein in chick embryo fibroblasts infected with the Rous sarcoma virus (11). Immunogold cytochemistry showed that over 90% of the caveolin in the plasma membrane is associated with caveolae and that small amounts of caveolin are also found in the Golgi apparatus (28). Independently, Kurzchalia et al. (17) showed that a protein of the same molecular weight as caveolin (designated VIP21) is prominent in Golgi-derived vesicles destined for the apical cell surface. Cloning of the cDNA, first for VIP21 (17) and then for caveolin (10), revealed that they are the same protein. The sequence predicts that it is an integral membrane protein synthesized without a leader peptide. The exact orientation of the protein in the plasma membrane is still not clear. Some evidence suggests that the protein forms a hairpin loop in the membrane such that both ends are in the cytoplasm (9). Other evidence (21) favors the view that it is a type II transmembrane protein.

The function of caveolin is not known. The association of this protein with the caveolar coat suggested that it might have a structural role in maintaining the shape of the organelle (28). In polarized epithelial cells, caveolin first associates with clusters of GPI-anchored membrane proteins in the Golgi apparatus (6, 21) before moving to the cell surface in transport vesicles (17). Therefore, caveolin may target GPI-anchored proteins and associated glycolipids to the api-

Address all correspondence to Eric J. Smart, Dept. of Cell Biology and Neuroscience, University of Texas Southwestern Medical Center, Dallas, Texas 75235.

1. *Abbreviations used in this paper*: DNP, dinitrophenol; GPI, glycosylphosphatidylinositol; PKC, protein kinase C.

© The Rockefeller University Press, 0021-9525/94/12/1185/13 $2.00

cal cell surface (17, 21). There is not any evidence, however, that plasmalemmal vesicles move from the cell surface to the Golgi apparatus as part of an internalization cycle.

Both the structure (28) and the function (7) of caveolae are absolutely dependent on membrane cholesterol. Exposure of membranes to sterol-binding drugs such as filipin cause the caveolar coat to disassemble, invaginated caveolae to become flat, and the GPI-anchored proteins to uncluster (28). Likewise, cells that are depleted of membrane cholesterol have unclustered GPI-anchored proteins, a reduced number of visible caveolae and potocytosis is impaired (7). These results are in agreement with the observation that caveolae have a much higher concentration of cholesterol than the surrounding plasma membrane (33).

Oxidation of cholesterol has been implicated as a risk factor in the development of atherosclerosis (14, 25). The essential role of cholesterol in caveola function suggests that it may be a plasma membrane domain that is especially sensitive to oxidative damage. To investigate this possibility, we used cholesterol oxidase to enzymatically oxidize fibroblast membrane cholesterol in situ. Surprisingly, this treatment caused caveolin to migrate to the Golgi region of the cell without there being a change in the number of caveolae. Caveolin recycles back to the plasma membrane after cholesterol oxidase is removed from the media and the level of oxidized cholesterol in the membrane declines.

Materials and Methods

Materials

Dulbecco's modified Eagle's medium, glutamine, trypsin-EDTA, and penicillin/streptomycin were from Gibco Laboratories (Grand Island, NY). Fetal calf serum was from Hazleton Research Products, Inc. (Lenexa, KS). The analytical silica gel thin-layer chromatography plates and the following solvents were from J. T. Baker, Inc. (Phillipsburg, NJ): heptane, petroleum ether, ethyl ether, acetic acid, and 2-propanol. [^{3}H]acetate was obtained from DuPont (Wilmington, DE) with a specific activity of approximately 4.13 Ci/mmol. Trans-[^{35}S]-label was from ICN (Costa Mesa, CA). Cholesterol oxidase (*Nocardia erythropolis*), cholesterol and cholestenone were from Boehringer Mannheim Biochemicals (Indianapolis, IN). The sulfuric-dichromate spray was from Supelco Inc. (Bellefonte, PA). Protein A-Sepharose (CL-4B) was from Pharmacia (Alameda, CA). Antibodies were obtained from the following sources: anti-caveolin IgG (mAb 2234) was a gift from Dr. John Glenney (Glentech, Inc., Lexington, KY); rabbit anti-BiP IgG was from David Bole (University of Michigan, Ann Arbor, MI) (4); rabbit anti-galactosyltransferase IgG was from E. G. Berger (Physiologisches Institute Universitat Zurich, Switzerland) (3); goat anti-mouse IgG conjugated to peroxidase was from Organon Teknika Corp (West Chester, PA); goat anti-rabbit IgG conjugated to gold (10 nm) was from Biocell (Ted Pella, Redding, CA); mouse anti-dinitrophenol IgG was from Oxford Biomedical (Oxford, MI); goat anti-mouse IgG conjugated to gold (10 nm) was from Energy Beam Sciences (Agawam, MA). All other reagents were from Sigma Chem. Co. (St. Louis, MO).

Methods

Cell Culture. Cultured fibroblasts were derived from a skin biopsy obtained from a normal patient. Cells were grown in a monolayer and set up according to a standard format (12). On day zero, 2.5×10^5 cells were seeded into 100-mm Petri dishes with 3 ml of Dulbecco's modified Eagle's medium supplemented with penicillin, streptomycin, 10% (vol/vol) human lipoprotein deficient serum. Cells were fed with fresh medium on day 3 and day 5. Cells were labeled with 75 μCi of ^{3}H-acetate on day six and used on day 7.

Thin-layer Chromatography. The thin-layer chromatography experiments were carried out as previously described (22). Three confluent 100-mm dishes of fibroblasts were used for each sample. The labeled cells were washed extensively in PBS and then placed in 3 ml of buffer (DMEM, 20 mM Hepes, pH 7.4) before the indicated treatments. The caveolae then were isolated on sucrose gradients (see below). Each gradient fraction was adjusted to 1 ml final volume and treated with 30% taurodeoxycholate, 2 ml Dole reagent (2-propanol, 78%: heptane, 20%: water, 2%), and 1 ml of heptane. The samples were vortexed and spun in a table top centrifuge for 10 min (3000 *g*). The heptane phase (upper) contained lipids and was used for thin-layer chromatography. The aqueous phase (bottom) contained proteins and was used for immunoblots. The heptane phase was dried under N_2 and suspended in 50 μl of the solvent system (80:20:1; petroleum ether/ethyl ether/acetic acid). Pure cholesterol and pure cholestenone were dissolved in the solvent system and used as standards (5 μg/spot). The lipids were spotted onto a silica gel G plate and developed in the solvent system. Lipids were visualized by charring with sulfuric acid-dichromate and heating at 180°C for 10 min. Unlabeled cholesterol and cholestenone were added to each fraction to facilitate visualization. The appropriate spots were scraped and the amount of radiation quantified by liquid scintillation counting.

Caveolae Isolation. Caveolae were isolated as described by Sargiacomo and colleagues (31). Three confluent, 100-mm dishes of human fibroblasts (10 mg protein) were used for each sample. All of the solutions contained a cocktail of protease inhibitors consisting of: leupeptin (10 μM), benzamidine (0.5 mM), soybean trypsin inhibitor (10 μg/ml), pepstatin A (1 μg/ml), and PMSF (0.2 mg/ml). Each dish was washed briefly with MBS (25 mM MES, pH 6.5; NaCl, 0.15 M) at room temperature. MBS plus 0.02% EDTA was added to each dish for 10 min on ice. The cells were pelleted in a table top centrifuge for 5 min, 1400 *g*, 4°C. Cells were suspended with a pipette tip in 1.0 ml MBS containing 1% Triton X-100. The samples were incubated on ice for 20 min and then dounced 20× in a 1 ml tight dounce. The samples were diluted with an equal volume of 85% sucrose. The mixed material was placed at the bottom of a centrifuge tube (TH641; Sorvall Instruments, Newton, CT) and a 10–30% linear sucrose gradient was layered on top. The samples were centrifuged at 143,200 *g* for 4 h at 4°C. After centrifugation the gradient was fractionated in 0.65-ml fractions before analysis.

Triton Solubility. Three 100-mm dishes of confluent fibroblasts were used for each sample. Cells were grown 22 h in methionine-free media that contained 300 μCi of [^{35}S]methionine (sp act 1132 Ci/mmol), washed three times with DMEM and then incubated for 5 h in the presence of 50 μg/ml of cycloheximide. The cells were washed extensively in PBS and subjected to the indicated treatments, all in the presence of cycloheximide. Cells were released from the dish by incubating in MBS plus 0.02% EDTA for 10 min on ice. The cells were collected by centrifuging for 5 min, 1400 *g* at 4°C. The pellets were suspended in 1.0 ml of MBS plus 1% Triton X-100 and incubated on ice for 20 min. The samples were dounced 20 times and spun in a microfuge for 5 min, 16000 *g* at 4°C. The supernatant fraction was collected and designated as the Triton-soluble fraction. The pellet was suspended in MBS plus 1% Triton and designated the Triton-insoluble fraction. Caveolin was immunoprecipitated from each of these fractions as described below.

Immunoprecipitation of Caveolin. Protein A-Sepharose beads were first blocked by incubating them for 4 h at 4°C with human fibroblast cell lysate (200 μg/ml) plus 30 mg/ml of BSA in MBS buffer that contained 1% Triton X-100 and 60 mM octylglucoside (MBSD buffer). Blocked beads were used to pre-clear the Triton X-100 soluble and insoluble fractions that had been suspended in MBSD. Pre-cleared fractions were then incubated for 19 h at 4°C with a 1:400 dilution of mAb anti-caveolin before adding blocked, Protein A-Sepharose beads and incubating an additional 2 h at 4°C. Beads were removed by centrifugation, dissolved in sample buffer (18), and proteins separated by electrophoresis. The autoradiograph was exposed for 48 h.

Protease Protection. Two 100-mm dishes of confluent fibroblasts were used for each sample. Cells that had been preincubated for 5 h in the presence of 50 μg/ml of cycloheximide were washed extensively in PBS and subjected to the indicated treatments, all in the presence of cycloheximide. At the end of the treatments, cells were removed from the dish with Trypsin-EDTA. Cells were collected by centrifugation at 1400 *g* for 5 min and then washed in 5 ml of lysis buffer (1 mM $NaHCO_3$; 1 mM $MgCl_2$; 10 mM KCl; 5 mM Hepes, pH 7.5; 0.3 M sucrose). Cells were pelleted at 1400 *g* for 5 min and then suspended in 0.5 ml of ice cold lysis buffer. Cells were broken by douncing 20 times with a 1 ml type A dounce homogenizer. The appropriate samples were incubated with 300 μg of trypsin for 30 min on ice. Soybean trypsin inhibitor (300 μg) was then added and the sample was centrifuged for 1 min at 600 *g* to remove unbroken cells. The remaining suspension was centrifuged at 100,000 *g* for 60 min at 4°C. The pellet was suspended in lysis buffer and analyzed by immunoblotting.

Electrophoresis and Immunoblots. Protein concentrations were deter-

mined by the BioRad Bradford assay (5) or the BioRad D.C. assay (Bio-Rad Labs, Richmond, CA). Proteins were concentrated by trichloroacetic acid precipitation. Pellets were dissolved in sample buffer and heated at 95°C for 3 min before being loaded onto gels. Proteins were separated in a 12.5% SDS–polyacrylamide gel using the method of Laemmli (18). Separated proteins were then transferred to nylon by the method of Towbin (35). The nylon was blocked in TBST (20 mM Tris, pH 7.6; 137 mM NaCl; 0.5% Tween-20) plus 3% dry milk for 1 h at room temperature. Anti-caveolin mAb 2234 diluted 1/500 in TBST + 1% dry milk was added for 1 h at room temperature. After incubating with the primary antibody, the nylon was washed four times, 10 min each in TBST plus 1% dry milk. The secondary antibody (goat anti-mouse conjugated to horseradish peroxidase) was diluted 1/30,000 and added for 1 h at room temperature. The nylon was then washed and bands visualized using enhanced chemiluminescence.

Indirect Immunofluorescence. Cells grown on glass coverslips were washed three times with PBS. After the indicated treatment, the cells were washed in PBS and fixed for 45 min at room temperature either with 3% (wt/vol) paraformaldehyde in PBS or with a fixative that contained 3.7% paraformaldehyde, 70 mM Lysine-HCl, and 10 mM $NaIO_4$ in 20 mM MES buffered saline (pH 7.0). After fixation, the cells were rinsed with PBS and incubated in 100 mM NH_4Cl-PBS for 10 min at room temperature. Cells were permeabilized with 0.1% Triton X-100 for 7 min on ice and washed extensively in PBS. Cells were then incubated sequentially with PBS plus 0.5% BSA for 1 h at room temperature, anti-caveolin mAb 2234 diluted 1/350 in PBS plus 0.2% BSA for 1 h at room temperature and finally with 20 μg/ml FITC-goat anti-mouse IgG plus 0.2% BSA for 1 h at room temperature. Cells were washed three times with PBS after each incubation. To colocalize caveolin and galactosyltransferase, the primary antibody incubation contained a mixture of mAb 2234 and polyclonal anti-galactosyltransferase (1:350). The secondary antibody incubation contained a mixture of RITC-goat anti-mouse IgG and FITC-goat anti-rabbit IgG. The concentration of the individual antibodies in the mixtures was the same as when they were used alone. Cells were then washed briefly in distilled water and mounted in a 2.5% solution of 1,4-diazabicyclo-(2.2.2)octane. Cells were photographed using a Zeiss Photomicroscope III.

Immunoelectron Microscopy. Cells were washed quickly with EM buffer (100 mM sodium phosphate, pH 7.6, 3 mM KCl, 3 mM $MgCl_2$) and then fixed with 3% (wt/vol) paraformaldehyde plus 3 mM trinitrophenol in EM buffer for 45 min at room temperature. The cells were rinsed with EM buffer for 10 min and then incubated for 20 min with 100 mM NH_4Cl in EM buffer at 4°C. Cells were rinsed with EM buffer for 10 min and then incubated with EM buffer that contained 0.15% bovine serum albumin and 0.01% saponin for 30 min at 4°C. Samples were incubated either with anti-caveolin mAb 2234 (1/100) or control mAb 2001 (20 μg/ml), rinsed, and then incubated with 20 μg/ml goat anti-mouse IgG conjugated to dinitrophenol (DNP); all with EM buffer plus 0.15% BSA and 0.01% saponin. All antibody incubations were 1 h at 4°C. Cells were fixed with 2% glutaraldehyde in EM buffer and incubated with 100 mM NH_4Cl in EM buffer before post-fixation with 1% OsO_4 containing 1.5% potassium ferricyanide in 100 mM sodium phosphate (pH 7.6). Samples were then dehydrated, embedded in Eponate, sectioned and processed to localize DNP groups by immunogold labeling as previously described (26). Immunogold quantification was carried out using a modification of a previously described method (30). Briefly, electron microscopic negatives were obtained by randomly photographing 60 regions from 40 different cells in each experimental treatment. The negatives were enlarged using a hand held magnifier and the surface length of the cell, the number of caveolae and the number of gold particles were measured directly.

Results

Cholesterol oxidase converts plasma membrane cholesterol to cholestenone without penetrating the lipid bilayer and entering the cell (19). To determine how much of the surface cholesterol in a living human fibroblast was accessible to the enzyme, we first metabolically labeled the cholesterol with tritium by growing the cells for 16 h in the presence of 36 μM [^{3}H]acetate (4.13 Ci/mmol). We then incubated the cells in the presence or absence of 0.5 U/ml cholesterol oxidase for 1 h at 37°C. The radiolabeled lipids were extracted from the cell with organic solvents, separated by TLC, and measured with a liquid scintillation counter. Cholesterol oxidase reproducibly converted 5–7% of the total cellular cholesterol to cholestenone. 1–2 h after removal of the enzyme from the culture medium, all of the radiolabeled cholestenone disappeared from the cell.

Caveolae are easily isolated from cultured cells because they are insoluble in Triton X-100 and, as a consequence, can be separated from other membranes by flotation on a sucrose gradient (31). We used this procedure to measure the amount of caveolin, [^{3}H]-cholesterol and [^{3}H]-cholestenone that was in caveolae before and after exposure of the cells to cholesterol oxidase. Untreated cells that had been homogenized in detergent were loaded on the bottom of a 10 to 30% sucrose gradient and centrifuged at 143,200 *g* for 4 h (Fig. 1 *A*). Immunoblots (Fig. 1 *A*, *Immunoblot*) showed that the majority of the caveolin was in fraction 10, which is well separated from the starting material in fraction 14. Fraction 10 contained only 6% of the total [^{3}H]-cholesterol (Fig. 1 *A*, ■), with the remainder in fractions 12–14. [^{3}H]-cholestenone was not present in any of the fractions (Fig. 1 *A*, ○). A dramatically different profile was seen after cholesterol oxidase treatment (Fig. 1 *B*). Virtually all of the [^{3}H]-cholesterol in fraction 10 (Fig. 1 *B*, ■) had been replaced by [^{3}H]-cholestenone (Fig. 1 *B*, ○). This was the exclusive location of oxidized cholesterol in these cells. More remarkably, caveolin was no longer in fraction 10 (Fig. 1 *B*, *Immunoblot*) but remained in the starting material (Fig. 1 *B*, *Fraction 14*). The quantitative conversion of the cholesterol in fraction 10 to cholestenone suggests that all of the oxidase-sensitive cholesterol in a living fibroblast is in the caveolae.

The caveolin may have remained in the starting material after cholesterol oxidase treatment because oxidized sterols render the protein soluble in Triton X-100 (Fig. 2). To test this idea, we first grew cells overnight in [^{35}S]methionine to metabolically label caveolin. Protein synthesis was stopped by adding cycloheximide to the media for 5 h and the cells were incubated in the presence or absence of 0.5 U/ml cholesterol oxidase for 1 h at 37°C. We then homogenized the cells in Triton X-100, separated the soluble (Fig. 2, *Triton Soluble*) and insoluble (Fig. 2, *Triton Insoluble*) material by centrifugation, and immunoprecipitated each fraction with mAb anti-caveolin IgG. All of the caveolin in untreated cells was in the insoluble fraction (Fig. 2, *NT*). After 60 min of cholesterol oxidase treatment, however, all of the caveolin was in the soluble fraction (Fig. 2, *CO*). Removal of the cholesterol oxidase from the culture medium caused a progressive return of caveolin to the insoluble fraction (Fig. 2, *chase*). 90 min after removal of oxidase, all of the caveolin was Triton insoluble (Fig. 2, *90 min*). Separate experiments showed that cholestenone disappeared from the cells within 60 min after cholesterol oxidase was removed from the medium (data not shown). We observed a quantitative (Fig. 2, compare band intensities) return of the Triton soluble caveolin to the insoluble fraction after cholesterol oxidase was removed from the media even though protein synthesis was blocked during this time.

Caveolin Reversibly Moves to the Golgi Apparatus

These results suggested that cholesterol oxidase caused the caveolin to leave the caveolae without changing the physical integrity of the caveolar membrane. Indirect immunofluores-

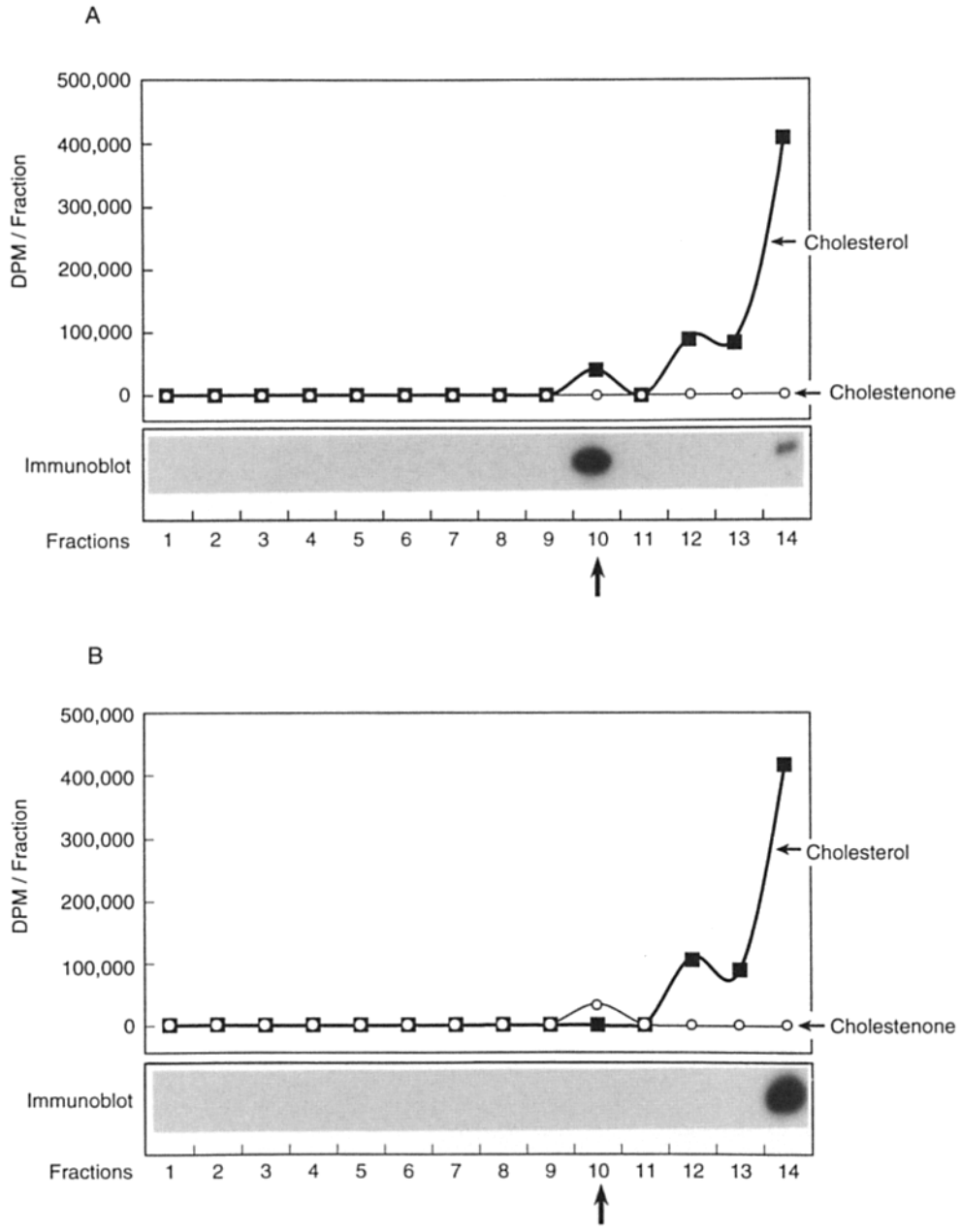

Figure 1. Distribution of cholesterol, cholestenone and caveolin in caveolae isolated from either untreated (*A*) or cholesterol oxidase-treated (*B*) cells. Human fibroblasts were incubated for 1 h at 37°C in the presence of either medium alone (*A*) or medium that contained 0.5 U/ml of cholesterol oxidase (*B*). Both sets of cells were solubilized in 1% Triton X-100 and caveolae isolated by flotation in a sucrose gradient. Fourteen fractions from the gradient were analyzed for the presence of caveolin (*Immunoblot*), cholesterol (■) and cholestenone (○) as described in Materials and Methods. The arrow indicates the caveolae fraction.

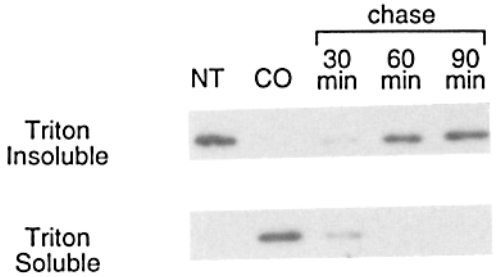

Figure 2. Effects of cholesterol oxidase on the Triton X-100 solubility of caveolin. Human fibroblasts were incubated in the presence of trans-[^{35}S]-label overnight, washed and further incubated in cold media that contained 50 μg/ml of cycloheximide for 5 h. They were then incubated for 1 h in the presence of either medium alone (*NT*) or medium that contained 0.5 U/ml of cholesterol oxidase (*CO* and *chase*). One set of cholesterol oxidase treated cells (*chase*) was incubated further for the indicated time in medium that did not contain any enzyme. Cycloheximide was present during all incubations. After each treatment, cells were removed from the dish with 1% Triton X-100 and the soluble (*Triton soluble*) and insoluble (*Triton insoluble*) fractions separated by centrifugation. Caveolin was immunoprecipitated from each fraction as described in Materials and Methods.

cence (Fig. 3, *A*, *C*, and *E*) and immunogold electron microscopy (Fig. 3, *B*, *D*, and *F*) confirmed this interpretation. The anti-caveolin IgG immunofluorescence staining pattern of untreated cells is shown in Fig. 3 *A*. The caveolin was primarily on the surface, concentrated in patches along the edge and over the body of the cell (Fig. 3 *A*). Immunogold labeling showed that nearly all of the caveolin was associated with in-

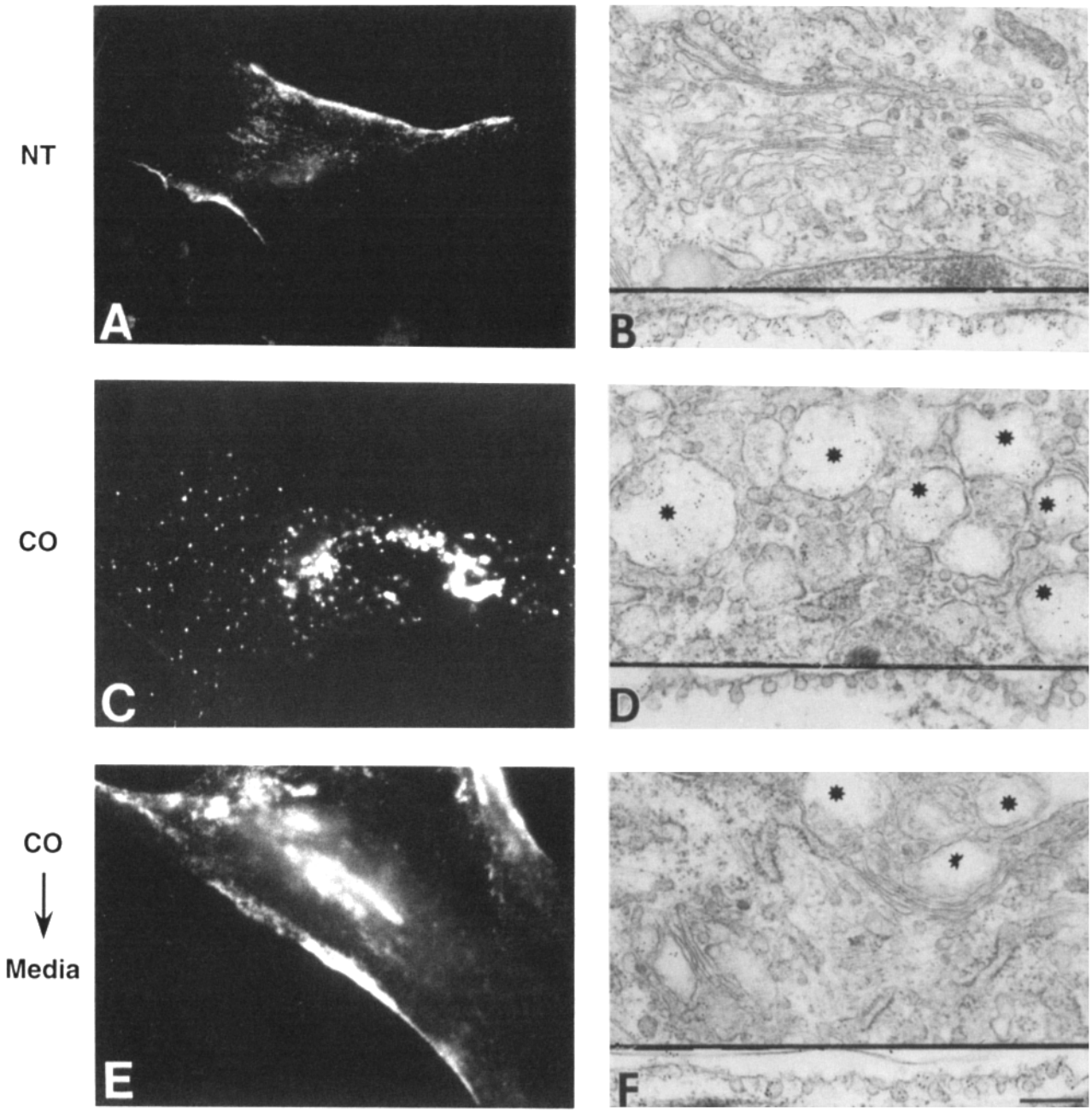

Figure 3. Immunofluorescence (*A*, *C*, and *E*) and immunogold (*B*, *D*, and *F*) localization of caveolin in untreated (*A* and *B*) and cholesterol oxidase-treated (*C–F*) cells. Human fibroblasts were incubated fo 1 h at 37°C in either medium alone (*A* and *B*) or medium that contained 0.5 U/ml of cholesterol oxidase (*C–F*). One set of cholesterol oxidase-treated cells (*E* and *F*) was incubated an additional 1 h in medium that did not contain any enzyme. At the end of the incubations, cells were processed to localize caveolin using either immunofluorescence (*A*, *C*, and *E*) or immunogold (*B*, *D*, and *F*) immunocytochemistry. Bar, (*a*, *c*, and *e*) 5.7 μm; (*b*, *d*, and *f*) 0.4 μm.

vaginated caveolae at the cell surface (Fig. 3 *B, bottom*) and that very little was present in the Golgi apparatus (Fig. 3 *B, top*). A 1-h treatment with cholesterol oxidase at 37°C dramatically changed this distribution. The caveolin now appeared in numerous vesicles that were concentrated near the nucleus of the cell (Fig. 3 *C*). Examination of treated cells with the electron microscope (Fig. 3 *D*) showed that in response to oxidation of cholesterol, cells accumulated numerous vesicles that were associated with the Golgi apparatus. The lumen of many of these vesicles was heavily labeled with anti-caveolin IgG-gold (Fig. 3 *D, top* [*]). There also was a dramatic reduction in the amount of gold in caveolae (Fig. 3 *D, bottom*) although caveolar morphology was unchanged. Quantification of the gold particles (Table I *A*) showed that cholesterol oxidase caused a ~60% decrease in the number of gold particles associated with caveolae. By contrast, there was only a 10% decline in the number of caveolae. Most of the caveolin returned to the cell surface (Fig. 3 *E*) after removal of cholesterol oxidase for 1 h at 37°C. The Golgi region returned to a more normal appearance, although some

Table I. Distribution of Caveolin After Cholesterol Oxidase Treatment

A. Cholesterol Oxidase at 37°C

Treatment	% Labeled caveolae	Total gold	Total caveolae	Gold/labeled caveola	Caveolae/ 10 μm
Control	47	1519	635	4.4	1.65
Cholesterol oxidase	29	632	632	3.6	1.47

B. Cholesterol Oxidase at 18°C then Warmed (↓) to 37°C

Treatment	% Labeled caveolae	Total gold	Total caveolae	Gold/labeled caveola
Control @ 18°C	65	5710	473	4.15
CO @ 18°C	41	4489	421	4.17
CO @ 18°C ↓ 37°C 30 min	48	3394	560	3.92
CO @ 18°C ↓ 37°C 90 min	31	1927	525	3.22

Human fibroblasts were subjected to the same conditions as described in the legend to Fig. 3 (for *A*) or Fig. 7 (for *B*) and then processed for quantification of anti-caveolin mAb gold as described.

of the *trans*-most cisternae appeared to be dilated (Fig. 3 *F, top* [*]). Very little immunogold was present in these cisternae. The quantity of caveolae-associated gold returned to normal levels (Fig. 3 *F, bottom*). The return of caveolin to caveolae paralleled the decline in membrane cholestenone.

Indirect immunofluorescence was used to determine if caveolin moved to the Golgi apparatus under conditions where protein synthesis was inhibited (Fig. 4). Cycloheximide was added to cells 5 h before the experiment and kept present throughout the incubations. Cells were either not treated (Fig. 4, *A* and *B*), incubated in the presence of cholesterol oxidase (Fig. 4, *C* and *D*), or exposed to cholesterol oxidase and then further incubated 1 h in the absence of the enzyme (Fig. 4, *E* and *F*). We then used immunofluorescence to colocalize caveolin (Fig. 4, *A, C,* and *E*) and the Golgi marker (3), galactosyltransferase (Fig. 4, *B, D,* and *F*). Normal surface membrane and Golgi apparatus staining was observed for the two markers in untreated cells (Fig. 4, *A* and *B*). After incubation in the presence of cholesterol oxidase, however, anti-caveolin IgG and anti-galactosyltransferase IgG staining were superimposed, indicating that caveolin had migrated to the Golgi apparatus (Fig. 4, *C* and *D*). Just as we observed with the electron microscope (Fig. 3), the Golgi apparatus appeared to be enlarged after cholesterol oxidation (compare Fig. 4, *B* with *D*). When the cholesterol oxidase was removed from the media and the cells incubated 1 h, anti-caveolin IgG staining was normal (Fig. 4, *E* and *F*), which indicates that caveolin had returned to caveolae. Therefore, cholesterol oxidase causes caveolin to move to the Golgi apparatus but the same molecules can return once the enzyme is removed.

The appearance of anti-caveolin IgG within the lumen of the Golgi cisternae after cholesterol oxidase treatment suggested that this integral membrane protein could move from the inside surface of the plasma membrane across the Golgi membrane. Therefore, we used two other standard methods to assess the topology of caveolin: antibody accessibility and protease protection.

At the proper temperature and concentration, digitonin will permeabilize the plasma membrane but leave the ER and Golgi membranes intact (2). We used indirect immunofluorescence with an antibody against the resident ER protein BiP (immunoglobulin heavy chain binding protein, [4]) to determine the conditions for selective permeabilization of human fibroblasts (Fig. 5, *D–F*). We found that 15 μg/ml of digitonin did not allow the antibody access to the BiP (Fig. 5 *E*) but treatment with 0.1% Triton X-100 gave a typical anti-BiP IgG staining pattern (Fig. 5 *D*). We then incubated cells in the presence of cholesterol oxidase and sequentially treated them with 15 μg/ml of digitonin and Triton X-100. These cells displayed a typical anti-BiP staining pattern (compare Fig. 5, *F* with *D*). When untreated cells were permeabilized with 15 μg/ml of digitonin and stained with anti-caveolin IgG, the staining pattern was normal (Fig. 5 *A*). By contrast, when we incubated the cells in the presence of cholesterol oxidase and then permeabilized them with digitonin, anti-caveolin IgG did not bind (Fig. 5 *B*). Antibody accessibility was restored after the cholesterol oxidase treated cells were sequentially treated with digitonin and Triton X-100 (Fig. 5 *C*).

Protease protection experiments also indicated that caveolin was crossing the ER-Golgi membrane system in cholesterol oxidase-treated cells (Fig. 6). Cells grown in cycloheximide to prevent protein synthesis were subjected to the different treatments and then gently homogenized in an isotonic buffer to preserve the integrity of intracellular organelles. We added either 300 μg/ml of trypsin or buffer alone directly to the homogenate and incubated the mixture for 30 min on ice. The proteins were separated by electrophoresis and immunoblotted with anti-caveolin IgG (Fig. 6). Untreated cells that were not exposed to the protease showed a distinct caveolin band (Fig. 6, *NT*). The addition of trypsin to untreated cell homogenates caused this band to disappear (Fig. 6, *NT+T*). Cholesterol oxidase-treated cells that were not exposed to trypsin also had a single immunoreactive band (Fig. 6, *CO*). In contrast to untreated

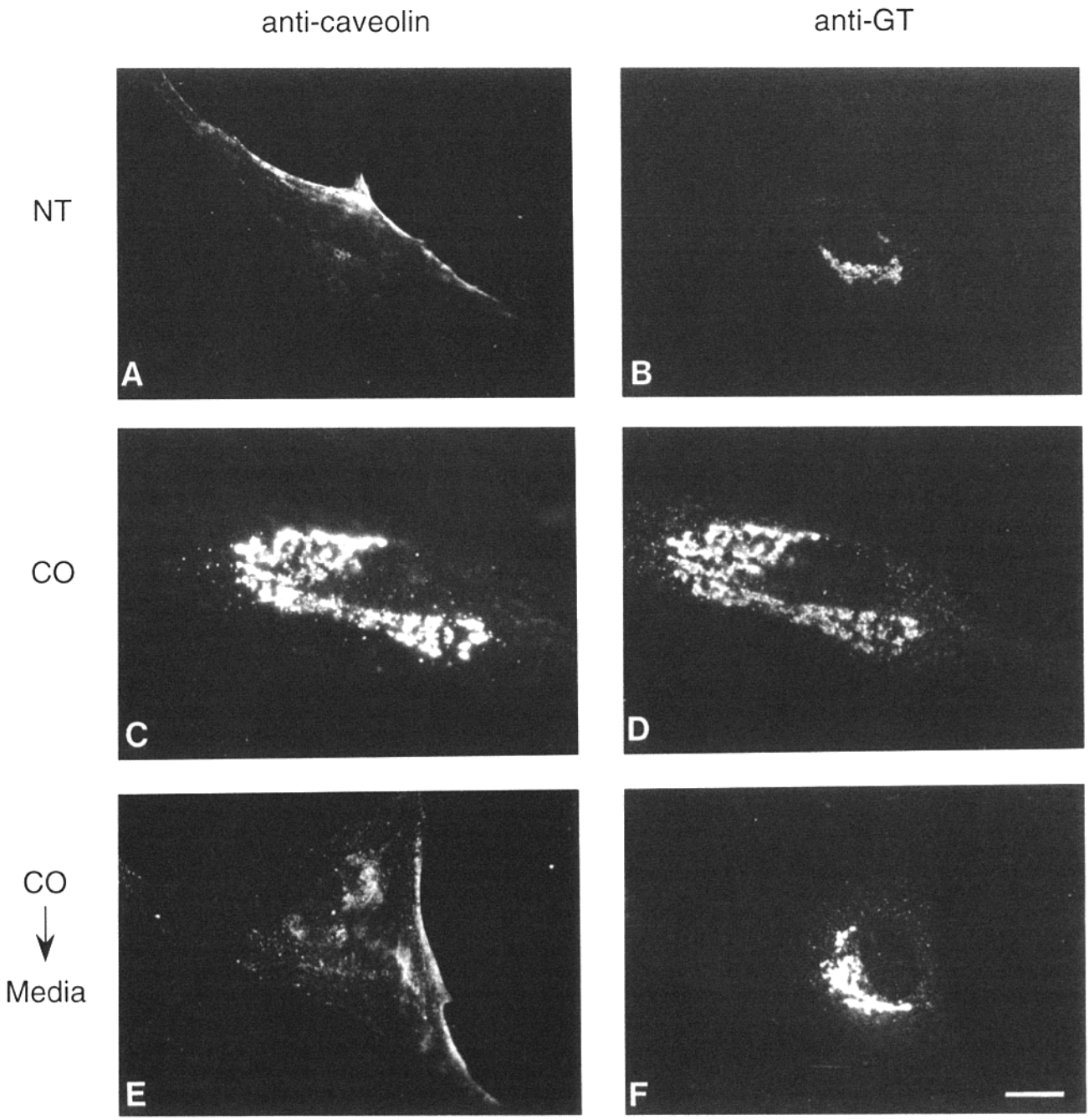

Figure 4. Reversible movement of caveolin to the Golgi apparatus in response to cholesterol oxidase. Human fibroblasts were incubated for 5 h in the presence of 50 μg/ml of cycloheximide. Cells were then either not treated (*A* and *B*), incubated in the presence of 0.5 U/ml of cholesterol oxidase for 1 h at 37°C (*C* and *D*), or incubated in the presence of cholesterol oxidase followed by incubation in the absence of the enzyme for 1 h at 37°C (*E* and *F*). Cycloheximide was present during all of the incubations. At the end of the incubations, the cells were fixed and processed to co-localize caveolin (*A*, *C*, and *E*) and the Golgi apparatus marker, galactosyltransferase (*B*, *D*, and *F*) by indirect immunofluorescence. All cells were fixed with periodate-lysine-paraformaldehyde fixative. Bar, 5.0 μm.

cells, this band was only slightly reduced in intensity when trypsin was added to the homogenate (Fig. 6, *CO+T*). The protected portion of caveolin was degraded when Triton X-100 was added to permeabilize membranes (Fig. 6, *CO+T+Triton*). Caveolin became completely protease sensitive after the cholesterol oxidase was removed from the medium and the cells incubated an additional 1 h (Fig. 6, *R+T*) even though protein synthesis was inhibited.

Low Temperatures and BFA Block Movement of Caveolin

We next carried out a series of experiments to identify the route that caveolin takes to get to the Golgi membrane. Since Golgi membrane and endosomal membrane traffic are both blocked at 18°C (8, 13), we incubated cells in the presence of cholesterol oxidase at this temperature and looked at the distribution of caveolin. Immunofluorescence showed (Fig.

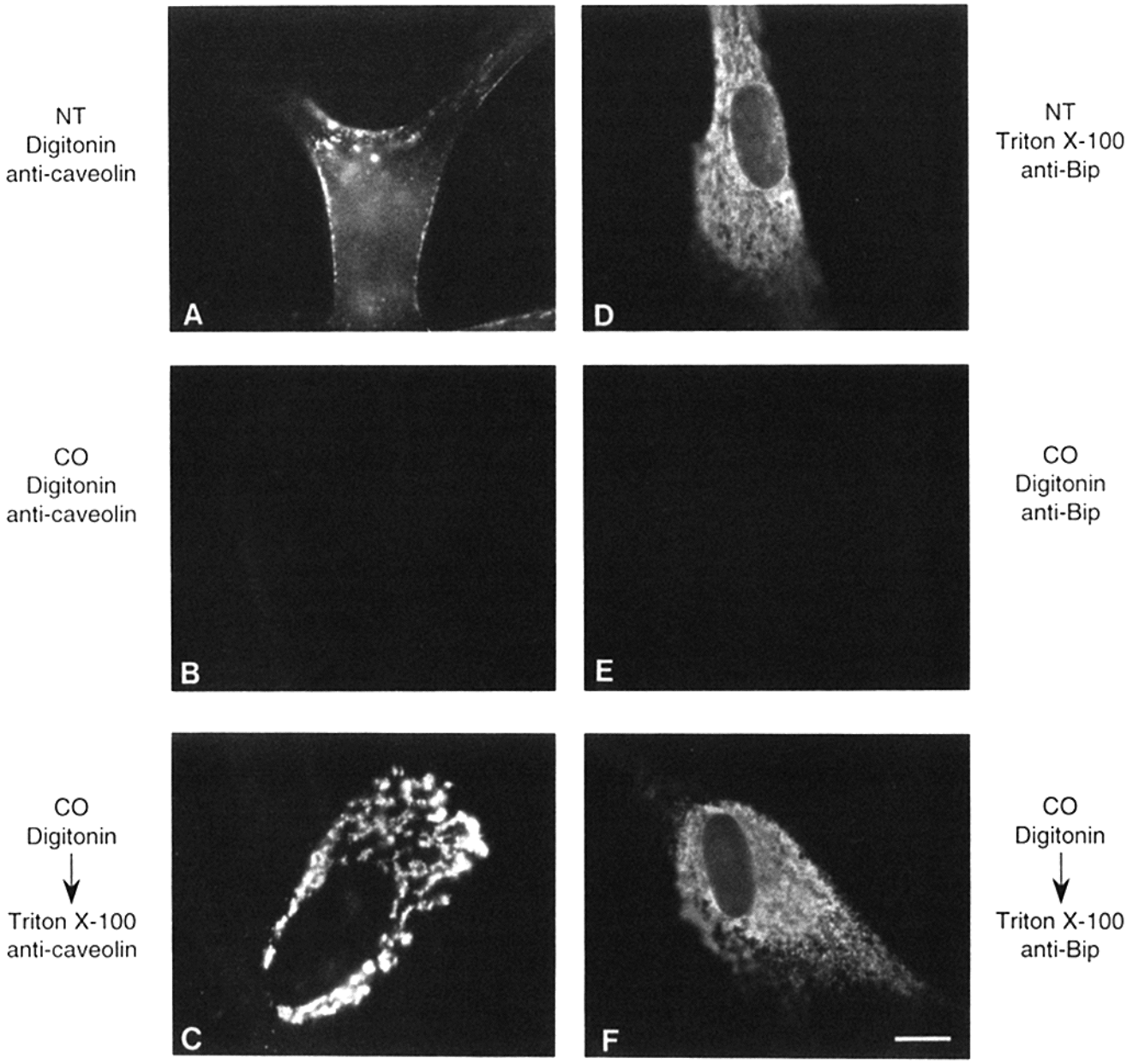

Figure 5. Effect of cholesterol oxidase on accessibility of caveolin to anti-caveolin IgG after digitonin permeabilization. Cells were incubated in the presence (*B*, *C*, *E*, and *F*) or absence (*A* and *D*) of cholesterol oxidase as described in Fig. 3. Cells stained with anti-BiP IgG (*D–F*) were permeabilized either with Triton X-100 (*D*), digitonin (*E*), or digitonin plus Triton X-100 (*F*). Cells stained with anti-caveolin IgG were permeabilized either with digitonin (*A* and *B*) or digitonin followed by Triton X-100 (*C*). All cells were fixed with periodate-lysine-paraformaldehyde fixative. Bar, 4.8 μm.

7) that most of the caveolin remained associated with the cell surface (compare Fig. 7, *A* with *B*). This temperature had no effect on the conversion of cholesterol to cholestenone (6%). When we shifted the 18°C-treated cells to 37°C for 30 min, almost all of the caveolin staining was in the Golgi apparatus (Fig. 7 *C*). 90 min after the shift, the caveolin was predominantly in vesicles near the cell center and in small vesicles distributed throughout the cell (Fig. 7 *D*).

We also found that once caveolin had migrated to the Golgi region it would not return to the cell surface at 18°C (Fig. 7). Caveolin was induced to move by treating the cells with cholesterol oxidase at 37°C. The cells were washed to remove the enzyme and further incubated 1 h at 18°C. Fig. 7 *E* shows that the caveolin remained in the Golgi region. Cellular cholestenone levels also remained constant during the incubation. By contrast, caveolin promptly returned to the cell surface when cells were incubated at 37°C for 1 h (Fig. 7 *F*).

We took advantage of the 18°C block and used immunogold labeling to follow caveolin from the cell surface to the Golgi region after shifting the temperature to 37°C (Fig. 8). Incubating cells at 18°C in the absence of cholesterol oxidase had no effect on the amount of anti-caveolin specific immunogold in either the Golgi apparatus (Fig. 8 *A*)

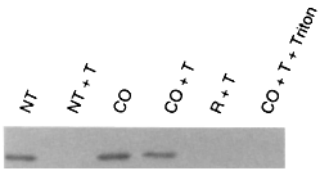

Figure 6. Effect of cholesterol oxidase on trypsin sensitivity of caveolin. Human fibroblasts that had been preincubated in the presence of 50 μg/ml of cycloheximide for 5 h were incubated either; in the absence of cholesterol oxidase (*NT*), in the presence of 0.5 U/ml of cholesterol oxidase (*CO*) for 1 h, or in the presence of cholesterol oxidase for 1 h followed by an additional 1 h in medium alone (*R*). Cells were homogenized as described in Materials and Methods and treated with 300 μg/ml of trypsin (*NT + T, CO + T, R + T*, and *CO + T + Triton*) for 30 min on ice. One set of homogenates from cholesterol oxidase treated cells was mixed with 0.1% Triton X-100 (*CO + T + Triton*) to allow trypsin access to the sequestered protein. After each treatment, the presence of caveolin was determined by immunoblot as described in Materials and Methods.

or the ER compartments (Fig. 8 *B*). With cholesterol oxidase present at this temperature, however, there was a substantial amount of immunogold associated with the rough ER (Fig. 8 *D* [*]) while the amount of gold label in the Golgi region remained unchanged (Fig. 8 *C*). Cells shifted to 37°C for 30 min had an increased amount of immunogold in the ER (Fig. 8 *F*) with a pronounced shift in distribution towards the smooth ER (Fig. 8 *F* [*]). Smooth ER could be recognized because often it was in continuity with the rough ER (Fig. 8, *F* and *H*; arrows) and the two ER compartments both contained a similar flocculent material in the lumen. Heavily labeled, dilated smooth ER was also found associated with the Golgi apparatus (Fig. 8 *E* [*]). After 90 min at 37°C, rough ER labeling declined (Fig. 8, *G* and *H*) but there was still good labeling of both smooth ER (Fig. 8 *H*) and Golgi-associated compartments (Fig. 8 *G*).

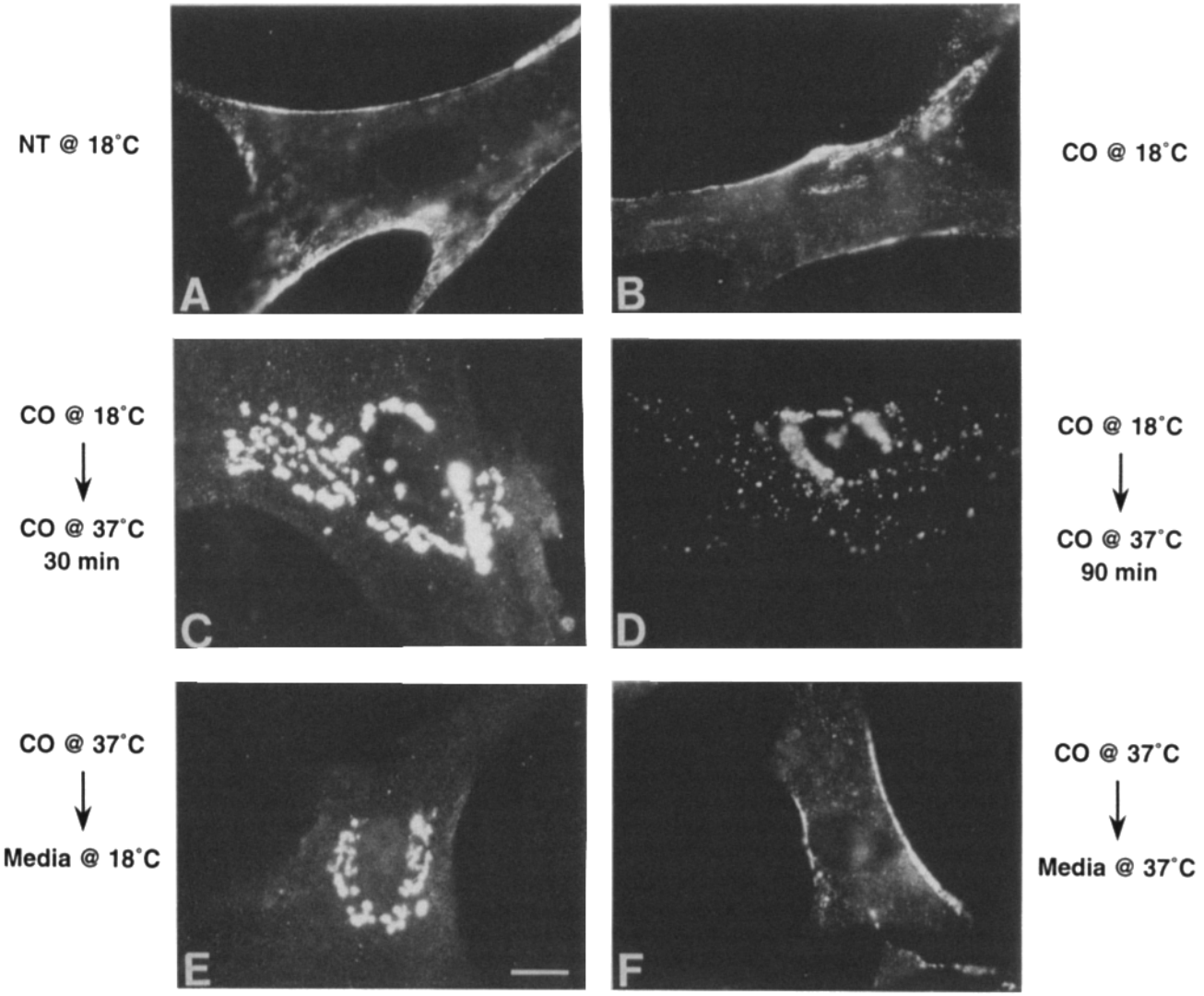

Figure 7. Effect of temperature on the distribution of caveolin in cholesterol oxidase treated cells. Human fibroblasts were incubated under the following conditions: (*A*) no cholesterol oxidase at 18°C; (*B*) 0.5 U/ml cholesterol oxidase at 18°C; (*C*) cholesterol oxidase at 18°C followed by cholesterol oxidase at 37°C for 30 min; (*D*) cholesterol oxidase at 18°C followed by cholesterol oxidase at 37°C for 90 min; (*E*) cholesterol oxidase at 37°C followed by medium alone at 18°C; (*F*) cholesterol oxidase at 37°C followed by medium alone at 37°C. At the end of the incubations, the cells were fixed and processed to localize caveolin by indirect immunofluorescence. Bar, 5.7 μm.

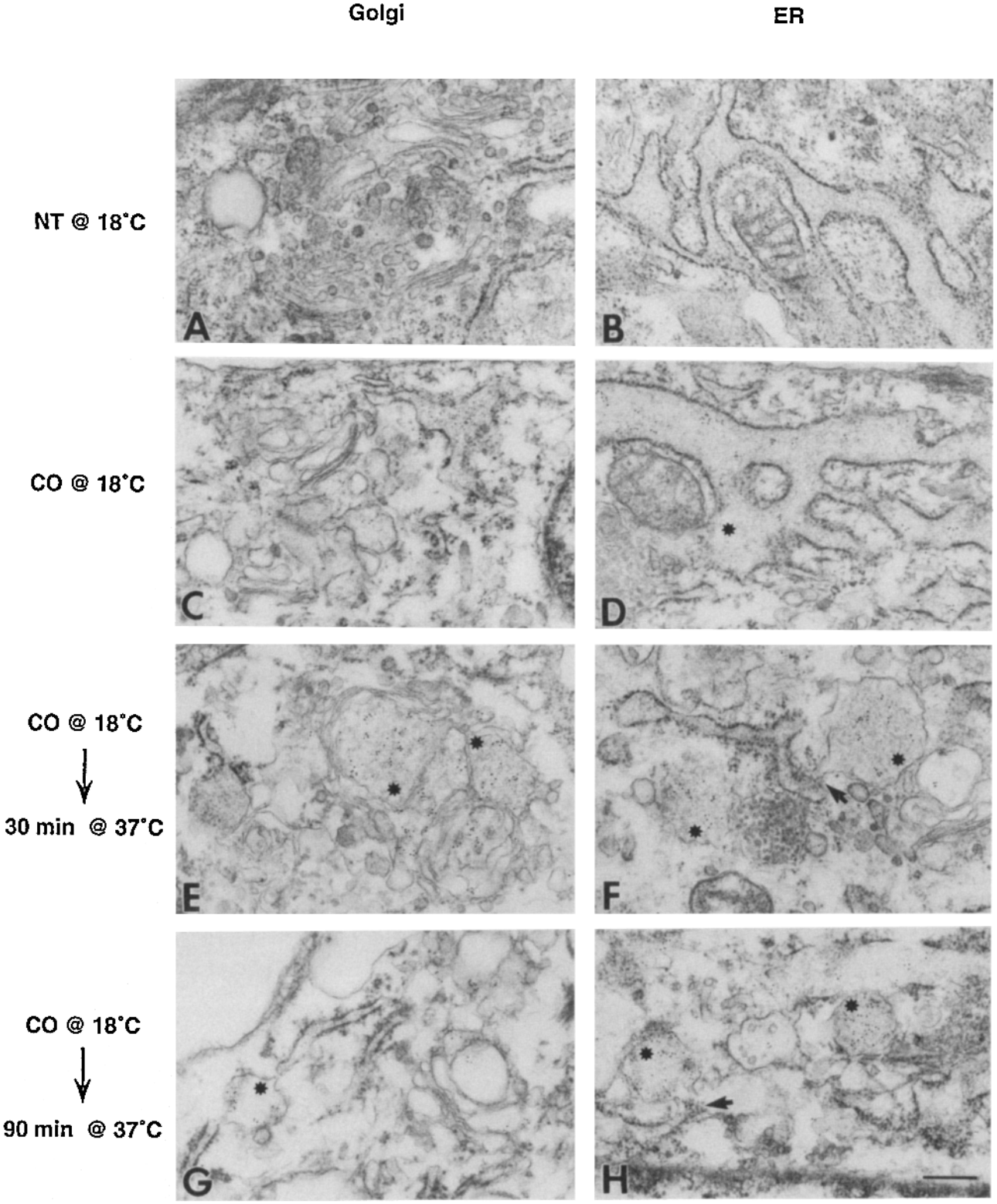

Figure 8. Immunogold localization of caveolin during its migration to the Golgi region of the cell in cholesterol oxidase treated cells. Human fibroblasts were either incubated in the presence (*C* and *D*) or absence (*A* and *B*) of 0.5 U/ml of cholesterol oxidase at 18°C or they were incubated in the presence of cholesterol oxidase at 18°C and then warmed to 37°C in the presence of cholesterol oxidase for the indicated time (*E–H*). At the end of the incubations, cells were fixed and processed for immunogold localization of caveolin as described. Representative areas of the Golgi region (*A*, *C*, *E*, and *G*) and ER (*B*, *D*, *F*, and *H*) compartments are shown for each treatment. Bar, 0.4 μm.

Quantitative electron microscopy confirmed these visual results (Table I *B*). Incubation in the presence of cholesterol oxidase at 18°C alone caused a 12% decline in the amount of immunogold that was associated with caveolae. After the temperature was shifted to 37°C, there was a progressive loss of caveolin from caveolae until at 90 min 70% had migrated away from this compartment. The dispersed arrangement of the ER in fibroblasts made it impossible to determine quantitatively if all of the caveolin had moved to the ER-Golgi compartment.

These results suggest that the rough ER may be involved in the movement of caveolin to the Golgi region of the cell. If this is the pathway, then brefeldin A (BFA) should block the accumulation of caveolin in the Golgi area because this drug disrupts membrane traffic between ER and Golgi compartments (20). Incubation of human fibroblasts in the presence of BFA had no effect on the distribution of caveolin (Fig. 9 *A*). When we switched these cells to medium that contained cholesterol oxidase and BFA (Fig. 9 *B*), anti-caveolin IgG labeling at the cell surface markedly declined. Instead, the staining pattern appeared as small, thin tubules that were diffusely distributed throughout the cell. When the BFA was removed in the presence of cholesterol oxidase, the caveolin migrated to the Golgi apparatus (Fig. 9 *C*). Caveolin returned to the cell surface after 1 h of incubation in the absence of both BFA and cholesterol oxidase (Fig. 9 *D*).

Discussion

Previous immunogold localization studies showed that caveolin was a component of the spiral coat that decorates the inside surface of the plasma membrane (28). The coat behaves as if it is constructed from integral membrane proteins (28), and the amino acid sequence of caveolin predicts that it belongs to this class of molecules (10, 17). The migratory behavior of caveolin now suggests that it is not a structural molecule of caveolae because the morphology of caveolae appears normal after most of the caveolin moves to the Golgi region. Therefore, caveolae can apparently exist in the absence of caveolin. This raises the possibility that there are tissue cells that have functional caveolae but no caveolin.

Caveolin and Membrane Cholesterol

The integrity of caveolae appears to depend on cholesterol (7). Previous electron microscopic studies have shown that caveolae are enriched in this sterol (33). We have also shown that depletion of intracellular cholesterol in MA104 cells causes a 10-fold reduction in the number of invaginated caveolae (29) and a significant inhibition of potocytosis (7). In addition, treatment of cells with cholesterol-binding drugs such as filipin causes invaginated caveolae to become flat (29). These results suggested that potocytosis and, consequently the opening and closing of the caveolae, are controlled by the lipid phase of the caveolar membrane.

Cholesterol oxidase has long been used to distinguish between plasma membrane and intracellular cholesterol pools (19). We can use the conversion of cholesterol to cholestenone by cholesterol oxidase to calculate that ~6–7% of the total cellular cholesterol is in caveolae. If 90% of the cholesterol is in the plasma membrane (19) and caveolae occupy 1–2% of this surface (30, 37), then caveolae membranes have

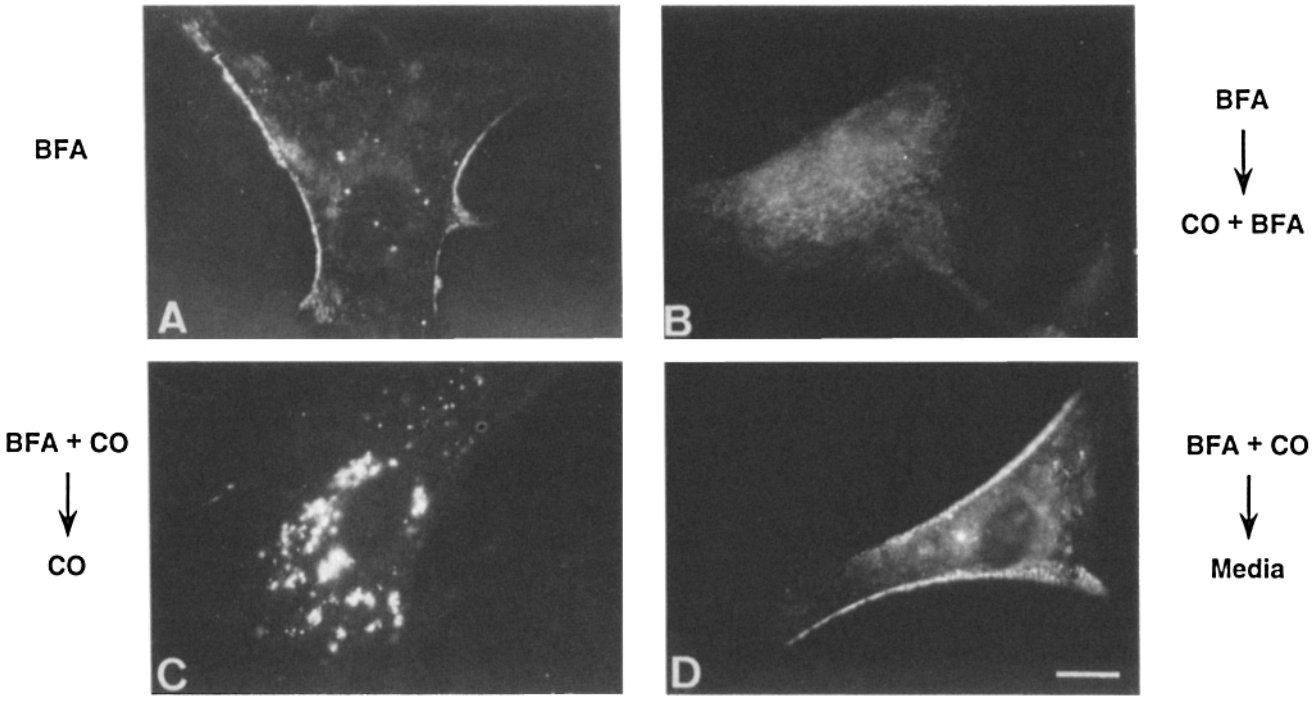

Figure 9. BFA prevents cholesterol oxidase-induced migration of caveolin to the Golgi region of the cell. Human fibroblasts were subjected to the following treatments at 37°C: (*A*) 1 h in 18 μM (BFA) (*B*) 1 h pretreatment with BFA followed by 1 h in 0.5 U/ml cholesterol oxidase plus BFA; (*C*) 1 h in BFA plus cholesterol oxidase followed by cholesterol oxidase alone for 1 h; (*D*) BFA plus cholesterol oxidase for 1 h followed by 1 h in medium alone. At the end of the incubations, the cells were fixed and processed to localize caveolin by indirect immunofluorescence. Bar, 5.7 μm.

four- to eightfold more cholesterol than the surrounding plasma membrane.

Our results suggest that caveolin may play a role in maintaining the proper cholesterol environment in the caveolae. Upon oxidation of caveolar cholesterol the caveolin leaves the plasma membrane and moves to the Golgi region of the cell. Ordinarily caveolin is not seen in the Golgi region because it spends most of the time on the cell surface. Oxidation of cholesterol perturbs this balance so that caveolin spends more time in the Golgi apparatus, which allows detection by indirect immunofluorescence. The cholestenone remains in the caveolae but the caveolae regain the normal amount of cholesterol as the caveolin returns to the plasma membrane. The fate of the cholestenone is not known. In polarized epithelial cells caveolin associates with GPI-anchored proteins, glycolipids, and cholesterol in the Golgi apparatus (6, 21). The caveolin–lipid complex then moves to the cell surface in Golgi-derived transport vesicles (17). The cycling of caveolin between the plasma membrane and the Golgi apparatus may allow the cell to specifically control the level of cholesterol in the caveolae and consequently their function.

Caveolin is not the only protein that migrates to the Golgi apparatus in response to oxysterols. The cytoplasmic oxysterol-binding protein (OSBP) also moves to the Golgi apparatus (27) when complexed with 25-hydroxycholesterol. OSBP is normally diffuse in the cytoplasm but after cells are incubated in the presence of 25-hydroxycholesterol it becomes associated with the Golgi apparatus. Our finding that caveolin moves to the Golgi apparatus suggests that the Golgi apparatus may have a general role to play in cholesterol homeostasis.

Caveolin Can Move from the Cell Surface to the Golgi Apparatus

The most remarkable observation in this study was the finding that caveolin, which is an integral membrane protein, can move to the Golgi apparatus region of the cell. The number of caveolae on the surface of the cell changed very little after cholesterol oxidase treatment, which may mean that the caveolin is not moving to the Golgi apparatus in plasmalemmal vesicles that have formed from caveolae. We also were unable to detect caveolin in any type of transport vesicle. While there are other explanations for the observations we have presented, two of the experimental results suggest that the ER has some role to play in the movement of caveolin to the Golgi apparatus: (*a*) oxidation of cholesterol at 18°C caused immunogold-detectable caveolin to first appear associated with the rough ER and this was followed by the progressive appearance of gold labeling in the Golgi apparatus after the cells were warmed to 37°C for various times (Fig. 8); (*b*) brefeldin A, which inhibits membrane traffic between the ER and Golgi apparatus (20), did not prevent the initial movement of caveolin into the cell but did prevent it from reaching the Golgi apparatus (Fig. 9). Further work will be required to determine exactly how the endoplasmic reticulum participates in caveolin transport to the Golgi apparatus.

The movement of caveolin to the Golgi region was reversible. Within one hour after cholesterol oxidase was removed from the medium, caveolin returned to the Triton X-100–insoluble fraction (Fig. 2) and to the cell surface (Fig. 4) even when protein synthesis was blocked with cycloheximide. This means that the same molecule of caveolin can travel between these compartments in a cycle. We do not know how caveolin returns to caveolae.

The identification of a novel cycling system for caveolin that is revealed by the oxidation of caveolar cholesterol supports previous findings that cholesterol is critical for the normal function of this membrane specialization (7, 29). The potential existence of a new pathway between the caveolae and the Golgi apparatus has broad implications for understanding the function of normal and diseased cells.

We would like to thank Mr. William Donzell for his important contribution in carrying out the immunofluorescence experiments. We are also grateful to Ms. Grace Liao for technical assistance.

This work was supported by grants from the National Institutes of Health, HL 20948, GM 43169, and GM 15631 and the Perot Family Foundation.

Received for publication 15 August 1994 and in revised form 7 September 1994.

References

1. Anderson, R. G. W., B. A. Kamen, K. G. Rothberg, and S. W. Lacey. 1992. Potocytosis: sequestration and transport of small molecules by caveolae. *Science (Wash. DC).* 255:410–411.
2. Balch, W. E., W. G. Dunphy, W. A. Braell, and J. E. Rothman. 1984. Reconstitution of the transport of protein between successive compartments of the Golgi measured by the coupled incorporation of N-acetylglucosamine. *Cell.* 39:405–416.
3. Berger, E. G., U. Muller, E. Aegerter, and G. J. Strous. 1987. Biology of galactosyltransferase: recent developments. *Biochem. Soc. Trans.* 15:610–613.
4. Bole, D. G., L. M. Hendershot, and J. F. Kearney. 1986. Posttranslational association of immunoglobulin heavy chain binding protein with nascent heavy chains in nonsecreting and secreting hybridomas. *J. Cell Biol.* 102:1558–1566.
5. Bradford, M. M. 1976. A rapid and sensitive method for the quantitation of microgram quantities of protein utilizing the principle of protein-dye binding. *Anal. Biochem.* 72:248–254.
6. Brown, D. A., and J. K. Rose. 1992. Sorting of GPI-anchored proteins to glycolipid-enriched membrane subdomains during transport to the apical cell surface. *Cell.* 68:533–544.
7. Chang, W.-J., K. G. Rothberg, B. A. Kamen, and R. G. W. Anderson. 1992. Lowering the cholesterol content of MA104 cells inhibits receptor mediated transport of folate. *J. Cell Biol.* 118:63–69.
8. Dunn, W. A., A. L. Hubbard, and N. N. J. Aronson. 1980. Low temperature selectively inhibits fusion between pinocytic vesicles and lysosomes during heterophagy of 125I-asialofetuin by the perfused rat liver. *J. Biol. Chem.* 255:5971–5978.
9. Dupree, P., R. G. Parton, G. Raposo, T. V. Kurzchalia, and K. Simons. 1993. Caveolae and sorting in the trans-Golgi network of epithelial cells. *EMBO (Eur. Mol. Biol. Org.) J.* 12:1597–1605.
10. Glenney, J. R. 1992. The sequence of human caveolin reveals identity with VIP21, a component of transport vesicles. *FEBS (Fed. Eur. Biochem. Soc.) Lett.* 314:45–48.
11. Glenney, J. R., and L. Zokas. 1989. Novel tyrosine kinase substrates from Rous Sarcoma Virus transformed cells are present in the membrane skeleton. *J. Cell Biol.* 108:2401–2408.
12. Goldstein, J. L., S. K. Basu, and M. S. Brown. 1983. Receptor-mediated endocytosis of LDL in cultured cells. *Methods Enzymol.* 98:241–260.
13. Haylett, T., and L. Thilo. 1991. Endosome-lysosome fusion at low temperature. *J. Biol. Chem.* 266:8322–8327.
14. Hubbard, R. W., Y. Ono, and A. Sanchez. 1989. Atherogenic effect of oxidized products of cholesterol. *Prog. Food & Nutr. Sci.* 13:17–44.
15. Kamen, B. A., and A. Capdevila. 1986. Receptor-mediated folate accumulation is regulated by the cellular folate content. *Proc. Natl. Acad. Sci. USA.* 83:5983–5987.
16. Kamen, B. A., A. K. Smith, and R. G. W. Anderson. 1991. The folate receptor works in tandem with a probenecid-sensitive anion carrier. *J. Clin. Invest.* 87:1442–1449.
17. Kurzchalia, T. V., P. Dupree, R. G. Parton, R. Kellner, H. Virta, M. Lehnert, and K. Simons. 1992. VIP21, a 21-kD membrane protein is an integral component of trans-Golgi-network-derived transport vesicles. *J. Cell Biol.* 118:1003–1014.

18. Laemmli, U. K. 1970. Cleavage of structural proteins during the assembly of the head of bacteriophage T4. *Nature (Lond.).* 227:680–685.
19. Lange, Y., M. H. Swaisgood, B. V. Ramos, and T. L. Steck. 1989. Plasma membranes contain half the phospholipid and 90% of the cholesterol and sphingomyelin in cultured human fibroblasts. *J. Biol. Chem.* 264: 3786–3793.
20. Lippincott-Schwartz, J., L. C. Yuan, J. S. Bonifacino, and J. D. Klausner. 1989. Rapid redistribution of Golgi proteins into the ER in cells treated with brefeldin A: Evidence for membrane cycling from Golgi to ER. *Cell.* 56:801–813.
21. Lisanti, M. P., Z. Tang, and M. Sargiacomo. 1993. Caveolin forms a hetero-oligomeric protein complex that interacts with an apical GPI-linked protein: Implications for the biogenesis of caveolae. *J. Cell Biol.* 123:595–604.
22. Moore, N. F., E. J. Patzer, Y. Barenholz, and R. R. Wagner. 1977. Effect of phospholipase C and cholesterol oxidase on membrane integrity, microviscosity and infectivity of vesicular stomatitis virus. *Biochemistry.* 16:4708–4715.
23. Palade, G. E. 1953. Fine structure of blood capillaries. *J. Appl. Physiol.* 24:1424.
24. Palade, G. E., and R. R. Bruns. 1968. Structural modulations of plasmalemmal vesicles. *J. Cell Biol.* 37:633–649.
25. Parthasarathy, S., D. Steinberg, and J. L. Witztum. 1992. The role of oxidized low-density lipoproteins in the pathogenesis of atherosclerosis. *Annu. Rev. Med.* 43:219–225.
26. Pathak, R. K., and R. G. W. Anderson. 1989. The use of dinitrophenol-IgG conjugates to detect sparse antigens by immunogold labeling. *J. Histochem. Cytochem.* 37:69–74.
27. Ridgway, N. D., P. A. Dawson, Y. K. Ho, M. S. Brown, and J. L. Goldstein. 1992. Translocation of oxysterol binding protein to Golgi apparatus triggered by ligand binding. *J. Cell Biol.* 116:307–319.
28. Rothberg, K. G., J. E. Heuser, W. C. Donzell, Y.-S. Ying, J. R. Glenney, and R. G. W. Anderson. 1992. Caveolin, a protein component of caveolae membrane coats. *Cell.* 68:673–682.
29. Rothberg, K. G., Y.-S. Ying, B. A. Kamen, and R. G. W. Anderson. 1990. Cholesterol controls the clustering of the glycophospholipid-anchored membrane receptor for 5-methyltetrahydrofolate. *J. Cell Biol.* 11: 2931–2938.
30. Rothberg, K. G., Y.-S. Ying, J. F. Kolhouse, B. A. Kamen, and R. G. W. Anderson. 1990. The glycophospholipid-linked folate receptor internalizes folate without entering the clathrin-coated pit endocytic pathway. *J. Cell Biol.* 110:637–649.
31. Sargiacomo, M., M. Sudol, Z. Tang, and M. P. Lisanti. 1993. Signal transducing molecules and GPI-linked proteins form a caveolin-rich insoluble complex in MDCK cells. *J. Cell Biol.* 122:789–808.
32. Simionescu, N. 1983. Cellular aspects of transcapillary exchange. *Physiol. Rev.* 63:1536–1560.
33. Simionescu, N., F. Lupu, and M. Simionescu. 1983. Rings of membrane sterols surround the openings of vesicles and fenestrae, in capillary endothelium. *J. Cell Biol.* 97:1592–1600.
34. Smart, E. J., D. C. Foster, Y.-S. Ying, B. A. Kamen, and R. G. W. Anderson. 1994. Protein kinase C activators inhibit receptor-mediated-potocytosis by preventing internalization of caveolae. *J. Cell Biol.* 124:307–313.
35. Towbin, H., T. Staehelin, and J. Gordon. 1979. Electrophoretic transfer of proteins from polyacrylamide gels to nitrocellulose sheets: procedure and some applications. *Proc. Natl. Acad. Sci. USA.* 76:4350–4354.
36. Yamada, E. 1955. The fine structure of the gall bladder epithelium of the mouse. *J. Biophys. Biochem. Cytol.* 1:445–458.
37. Ying, Y.-S., R. G. W. Anderson, and K. G. Rothberg. 1992. Each caveola contains multiple glycosyl-phosphatidylinositol anchored membrane proteins. *Cold Spring Harbor Symp. Quant. Biol.* 57:593–604.